Supporting Information

Single-neuron identification of chemical constituents, physiological changes and metabolism using mass spectrometry

Hongying Zhu[a,b,1], Guichang Zou[b,1], Ning Wang[b,1], Meihui Zhuang[a], Wei Xiong[b-e,2] and Guangming Huang[a,2]

a. CAS Key Laboratory of Urban Pollutant Conversion, School of chemistry and materials science, University of Science and Technology of China, 96 Jinzhai Road, Hefei, Anhui 230026, China
b. School of Life Sciences, University of Science and Technology of China, Hefei 230026, China
c. Neurodegenerative Disorder Research Center, University of Science and Technology of China, Hefei 230026, China
d. CAS Key Laboratory of Brain Function and Disease and Hefei National Laboratory for Physical Sciences at the Microscale, University of Science and Technology of China, Hefei 230026, China
e. Center for Excellence in Brain Science and Intelligence Technology, Chinese Academy of Sciences, Shanghai 200031, China

SI Methods

***Allium* cepa preparation and single-cell sampling.** *Allium* cepa bulbs were washed with Milli-Q-Plus ultra-pure water (Milipore, Bedford, MA, USA; resistance ≥ 18 MΩ/cm) to clean the surface of the epidermis. Then, the bulbs were cut longitudinally with a surgical scalpel. A layer of scale was selected and cut into a strip of between 4 and 6 cm^2. Intact monolayers of the inner and outer epidermal tissues on the concave surface were peeled away from the parenchymal tissue. The wet surface of the epidermis was used to mount the tissue to a glass slide for subsequent experiments.

Single-cell micropipette sampling was performed with a motorized micromanipulator (MP-285, Sutter Instrument, Novato, CA, USA) mounted on a universal stand (TMC Vibration Control, Gimbal Piston) next to an upright microscope (Olympus BX51WI, Olympus Optical, Tokyo, Japan). A schematic view of the single-cell sampling setup is shown in Fig. S1 A holder with a new capillary tip was attached to the micromanipulator at an angle of 30 degrees relative to the microscope sample stage. Initially, the micropipette tip was moved into the focal plane of the microscope. Before sampling, it was moved approximately 200 μm upwards to make room for the sample. Then, a microscope slide containing a slice of *Allium* cepa bulb epidermis was placed on the sample stage and brought to the focal plane. The cell of interest was centered in the field of view. At this point, the micropipette tip was carefully lowered and positioned near to the center of a single cell. Then, it was carefully inserted to a depth of ~2 μm to prevent contact with the adjacent cells underneath. After the insertion of the tip, the cytoplasm, driven by capillary action and turgor pressure, automatically entered the sampling device. When approximately 5-10 pL of cytoplasm had been withdrawn from the cell, the capillary was quickly removed from the slice and assayed by InESI-MS.

sEPSCs and sIPSCs recording. sEPSCs were recorded with a holding potential of -70 mV and PTX (100 μM), which was used to block the GABA and glycine receptors, diluted with aCSF. The EPSC internal recording solution (pH 7.2) contained 145 mM potassium gluconate, 5 mM HEPES, 5 mM Mg-adenosine triphosphate (ATP), 0.2 mM Na-guanosine 5′-triphosphate (GTP), and 10 mM ethylene glycol-bis(β-aminoethyl ether)-N,N,N′,N′-tetraacetic acid (EGTA). In addition, sIPSCs were assayed in a whole-cell configuration at -60 mV. Patch pipettes (3-5 MΩ) were filled with an intracellular solution containing 140 mM CsCl, 4 mM $MgCl_2$, 10 mM EGTA, 10 mM HEPES, 2 mM Mg-ATP, and 0.5 mM Na-GTP. Kynurenic acid (4 mM) was added to the incubation solution to block the Glu receptors. Experimental results were discarded if the series resistance varied by more than 15% or exceeded 25 MΩ, as previously described. An alternative pipette solution (APS) containing 185 mM NH_4HCO_3 and 80 mM NH_4Cl was used for subsequent sampling experiments, because the CPS contained too much HEPES and CsCl, resulting in intense ion suppression and salt effects during MS detection.

MS settings. Orbitrap MS: capillary temperature: 275 ℃, S-lens radio frequency (RF) level: 50%, mass resolution: 140,000, maximum inject time: 10 ms, and microscans: 1.

LTQ Velos Pro. MS: capillary temperature: 275 ℃, S-lens RF level: 42%, maximum injection time: 300 ms, and microscans: 1. Some chemical structure identifications were facilitated by tandem MS using LTQ Velos Pro. MS instruments based on collision-induced dissociation (CID) in helium (He) background gas at 30% energy. The commercial ESI source was removed before our experiments. The source voltage was set at 2 kV for conventional NanoESI.

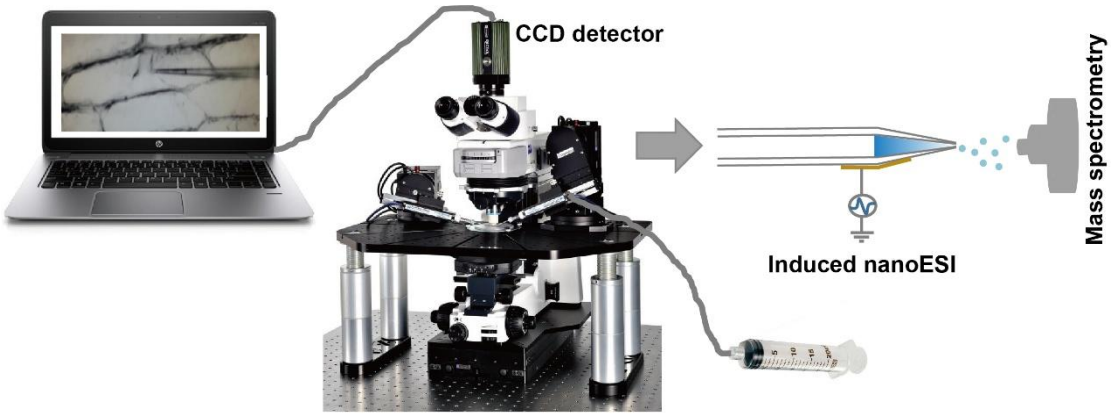

Fig. S1. Scheme diagram of the combination of capillary micro sampling and Induced NanoESI/MS (InESI/MS) for *Allium cepa* bull epidermal cells. Microscope was downloaded from KYS technology website.

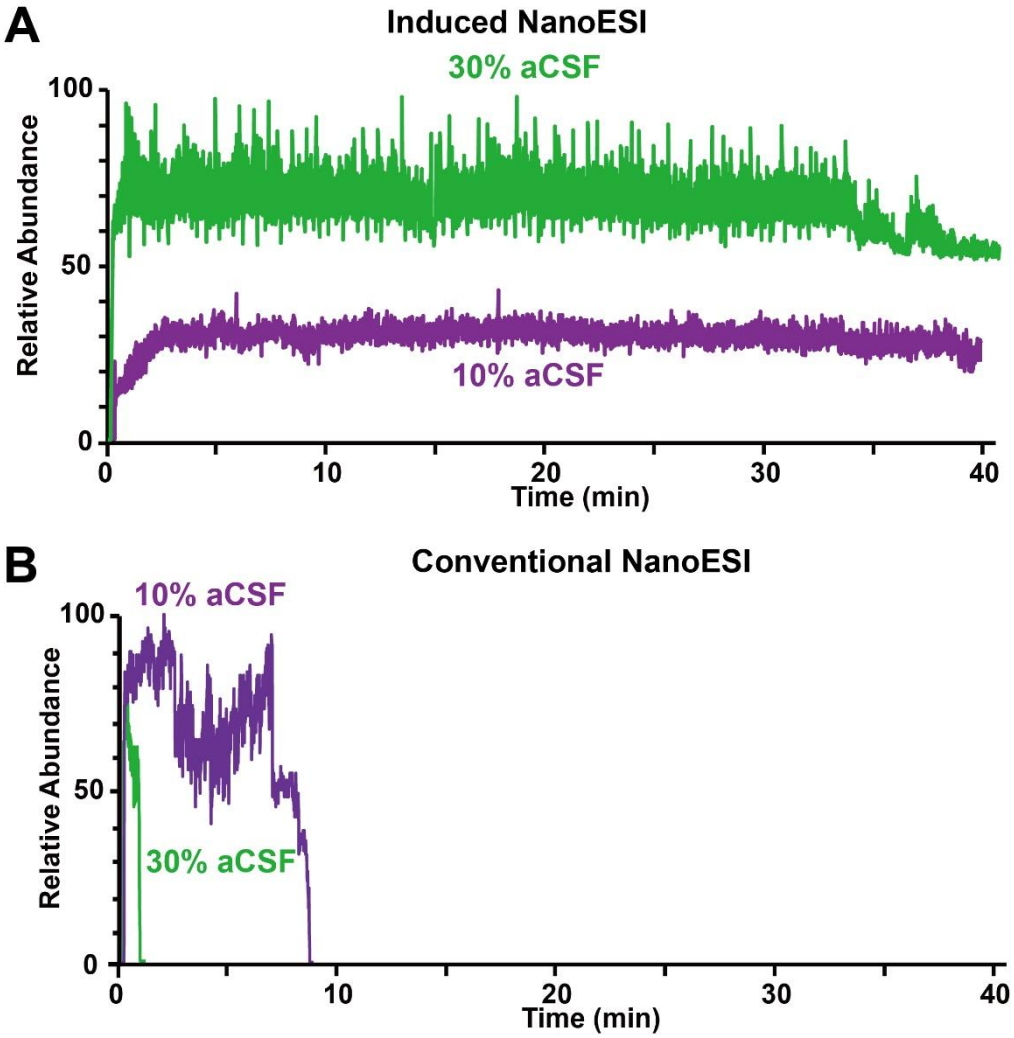

Fig. S2. InESI technique is ability to avoid clogging with electrolyte solutions at various concentrations. Typical signal duration of induced NanoESI *(A)* and conventional NanoESI *(B)* in 10% aCSF solution (green line) and 30% aCSF solution (purple line) diluted with NH_4HCO_3-NH_4Cl. For 10% aCSF solution diluted with NH_4HCO_3-NH_4Cl, the clogging of the spray emitter occurred within ~9 mins for conventional NanoESI. While with the same or higher concentration aCSF solution, MS signal for induced NanoESI remained stable for over 40 mins.

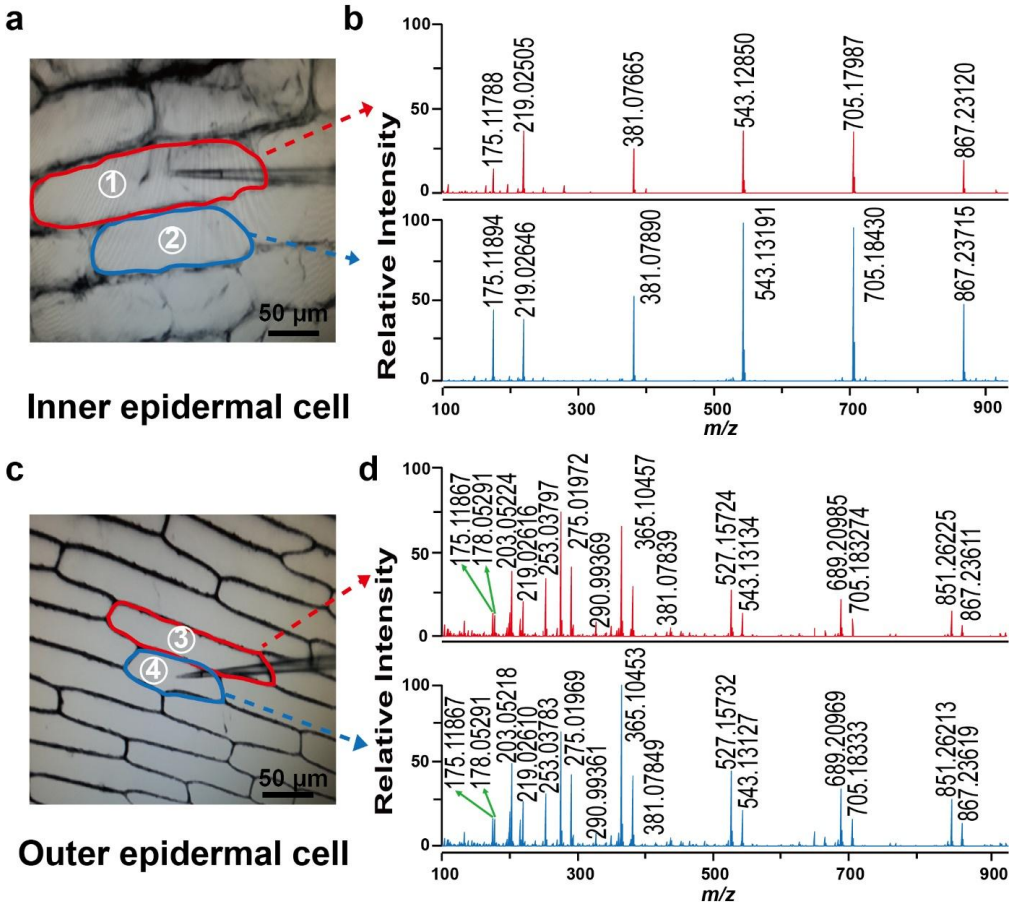

Fig. S3. InESI/MS measurement of epidermal cells from *Allium cepa* bulbs (*A* and *C*). Major metabolites of *Allium cepa* bull epidermal cells were identified (*B, D* and Table S1). A clear distinction between the inner and outer epidermal cells of *Allium cepa* was found (*B* and *D*). No significant difference was observed between adjacent inner epidermal cells (*B*) or between adjacent outer epidermal cells (*D*). However, more ions were found in the outer epidermal cells (Fig. S4 and Table S1). Even for the same type of chemical (hexose and oligosaccharides), different forms were observed to predominate in the inner (potassium adducts) and outer (sodium adducts) epidermal cells, implying that the sodium and potassium concentrations might vary from cell to cell. We also tested the stability of the MS spectra obtained from the cytoplasm of a single onion cell via InESI/MS (Fig. S5).

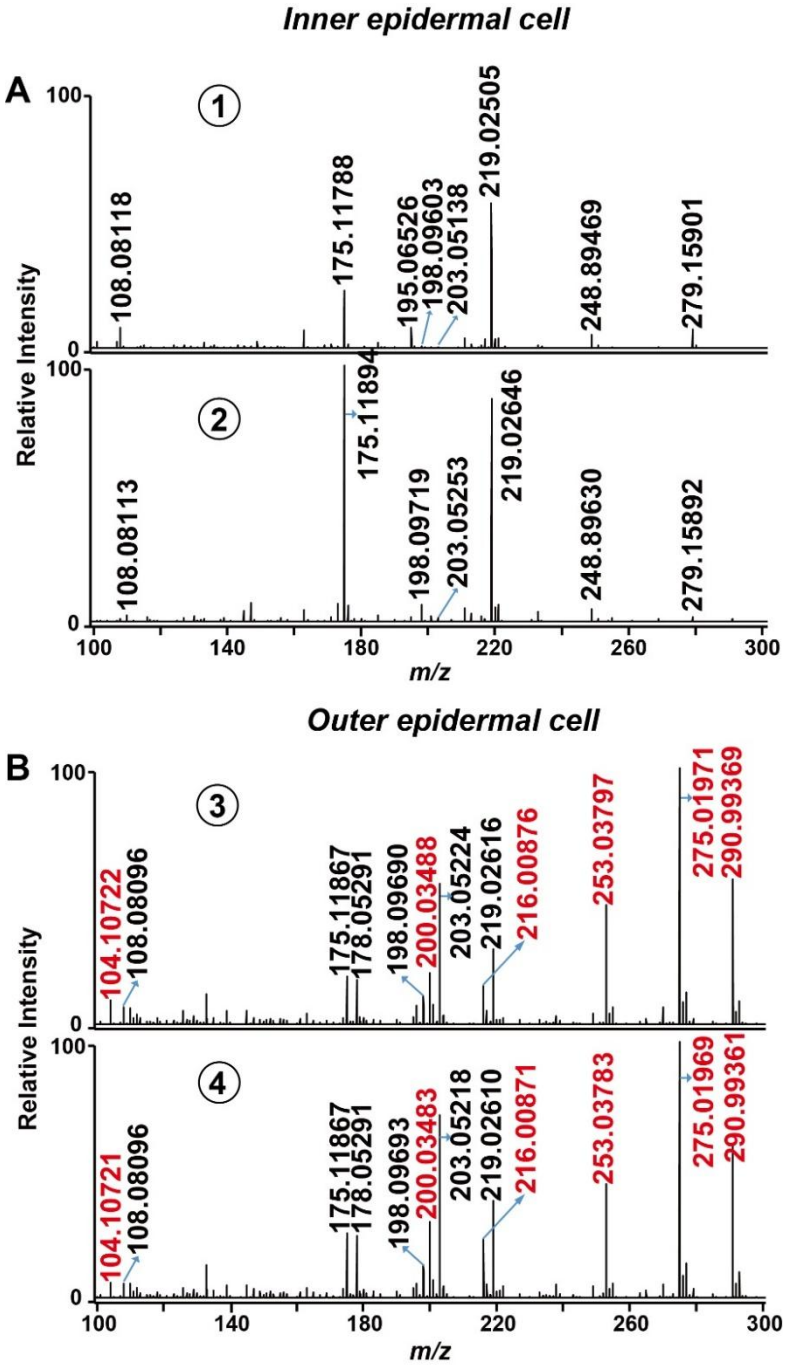

Fig. S4. Zoom in Fig. S3 from *m/z* 100 to 300. No significant difference was observed between adjacent inner epidermal cells (cell ① and ②) or between adjacent outer epidermal cells (cell ③ and ④). Some common metabolites were detected in both outer and inner epidermal cells. For cells from outer epidermal, more abundant ions (red characters in *B*) were found as Neurine ([neurine + H]$^+$, *m/z* 104.10722), N-formyl-L-methionine ([N-formyl-L-methionine + Na]$^+$, *m/z* 200.03488 and [N-formyl-L-methionine + K]$^+$, *m/z* 216.00876) and a sulfur-containing compound (protonated: *m/z* 253.03789, sodium adduct: *m/z* 275.01972 and potassium adduct: *m/z* 290.99370)

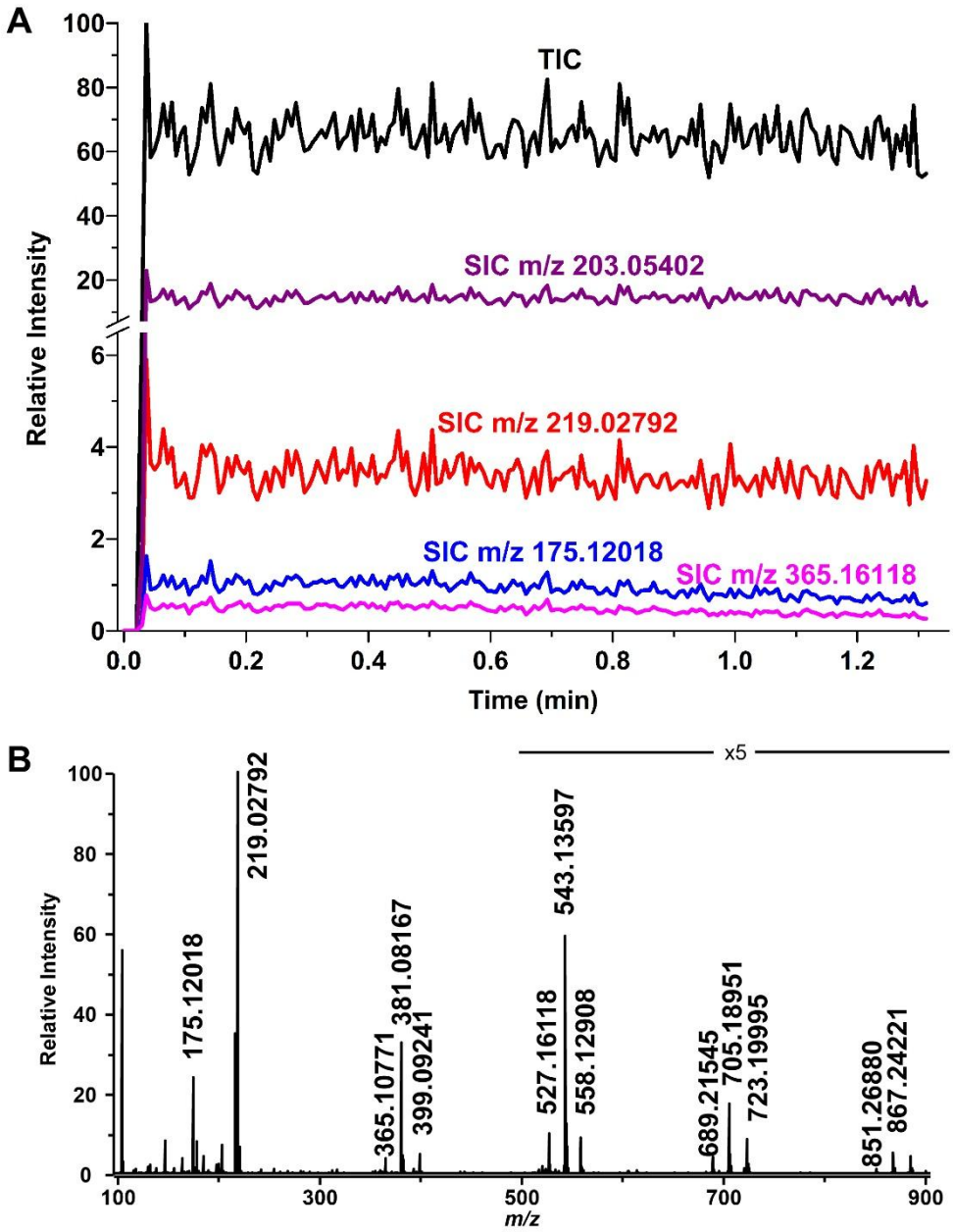

Fig. S5. Stability of MS spectra obtained by induced NanoESI/MS with cytoplasm of single onion cell. *(A)* Total ion chromatogram (TIC, black line) and selected ion chromatogram (SIC, purple line *m/z* 203.05402 [Hexose + Na]$^+$, red line *m/z* 219.02792 [Hexose + K]$^+$, blue line *m/z* 175.12018 [Arginine + H]$^+$, pink line *m/z* 365.16118 [Disaccharide + Na]$^+$). *(B)* Mass spectrum of the single onion cell.

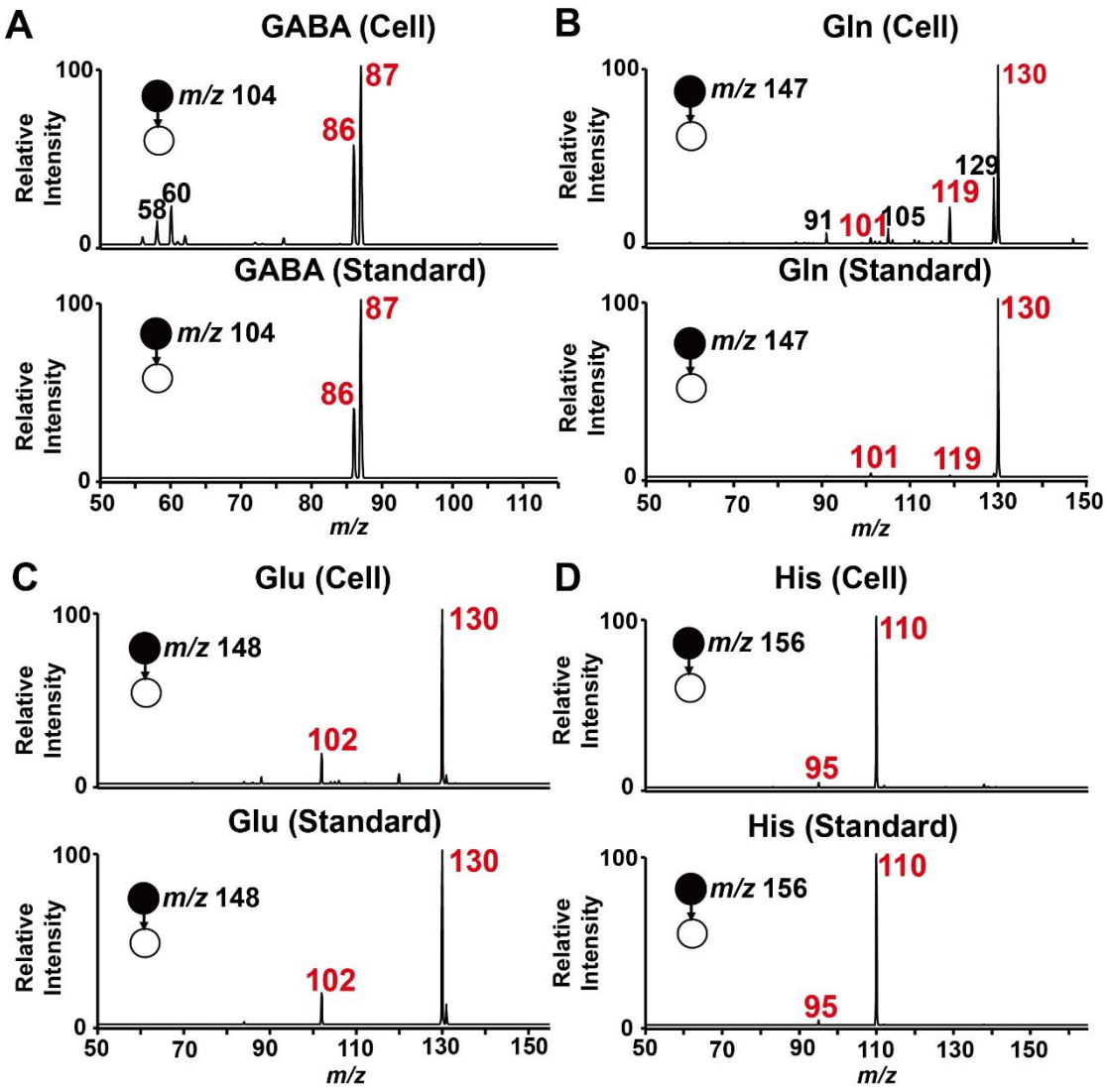

Fig. S6. Typical tandem mass (MS/MS) spectra for metabolites obtained from single neuron samples. The chemical assignments were verified by comparing MS/MS spectra to the ones obtained from commercially standards (*A*: GABA, *B*: Gln, *C*: Glu and *D*: His).

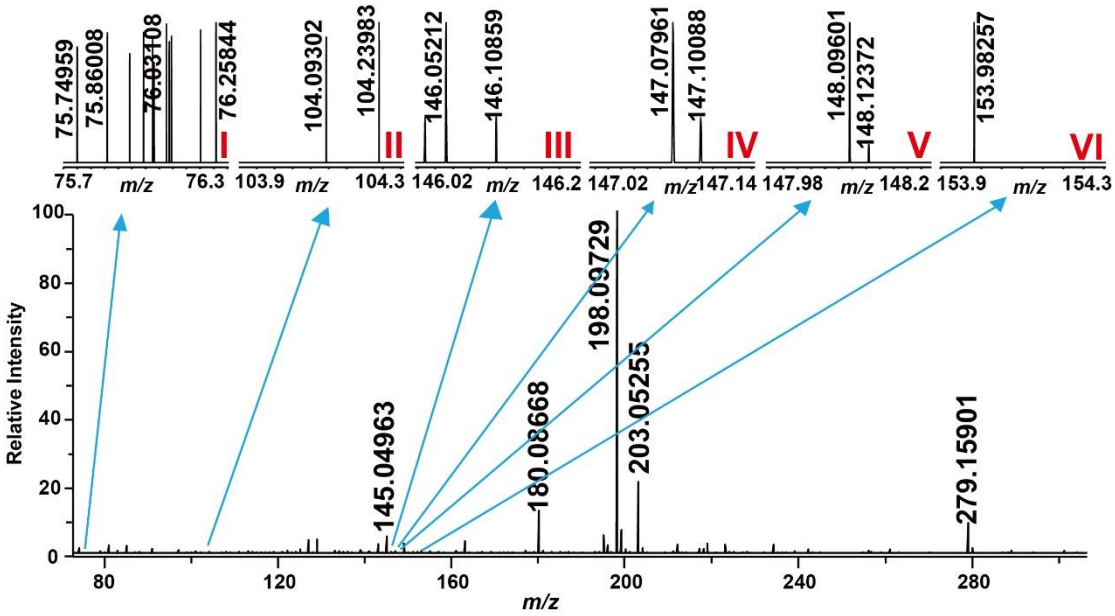

Fig. S7. The metabolites described in Fig. 2*b* (main text) were not observed in the mass spectrum of the control sample. The expanded views were mass spectra of different *m/z* range, which covered the *m/z* range of glycine (I), GABA and choline (II), acetylcholine (III), Gln (IV), Glu (V) and dopamine (VI), but none of the metabolites was seen. The control sample was obtained by applying negative pressure when the pipette tip was placed ~2 μm close to the neurons, then the extracellular fluid was drawn into the patch micro-pipette.

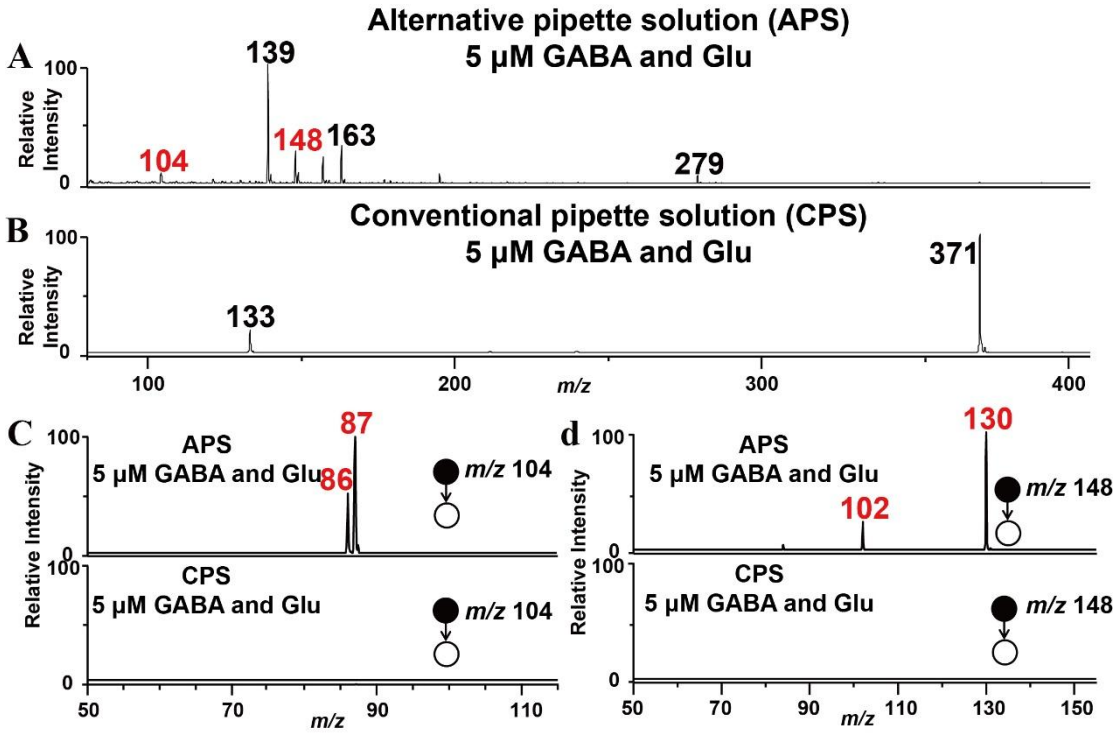

Fig. S8. Conventional pipette solution induced intensive ion suppression effect and salt effect demonstrated by spiked samples. Spiked GABA and Glu (5 μM each) clearly observed in alternative pipette solution (APS, *A*), with structures confirmed using MS/MS (top of *C* and *D*). However, with conventional pipette solution (CPS), spiked GABA and Glu (5 μM each) could be neither observed in mass spectrum (*B*) nor confirmed in MS/MS spectra (down of *C* and *D*).

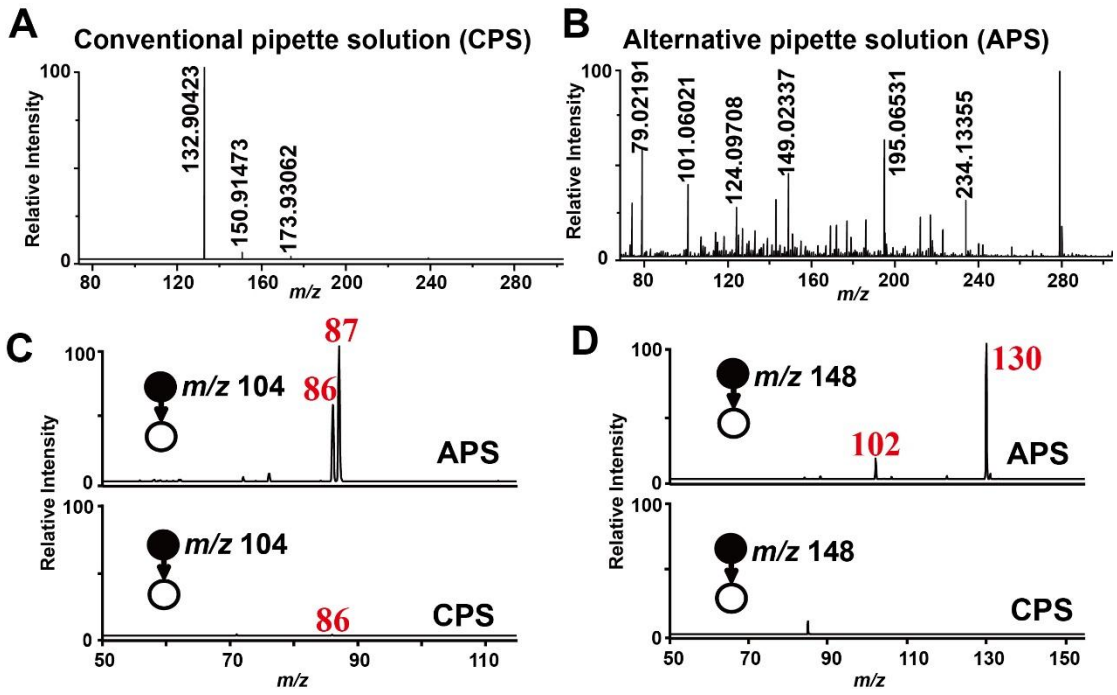

Fig. S9. Conventional pipette solution induced intensive ion suppression and salt effect for single neuron MS detection. The metabolites described in Fig. 2 (main text) were not observed in the mass spectrum when CPS was used (*A*, down of *C* and *D*). When APS solution was used, the neuron metabolites could be observed (*B*, top of *C* and *D*).

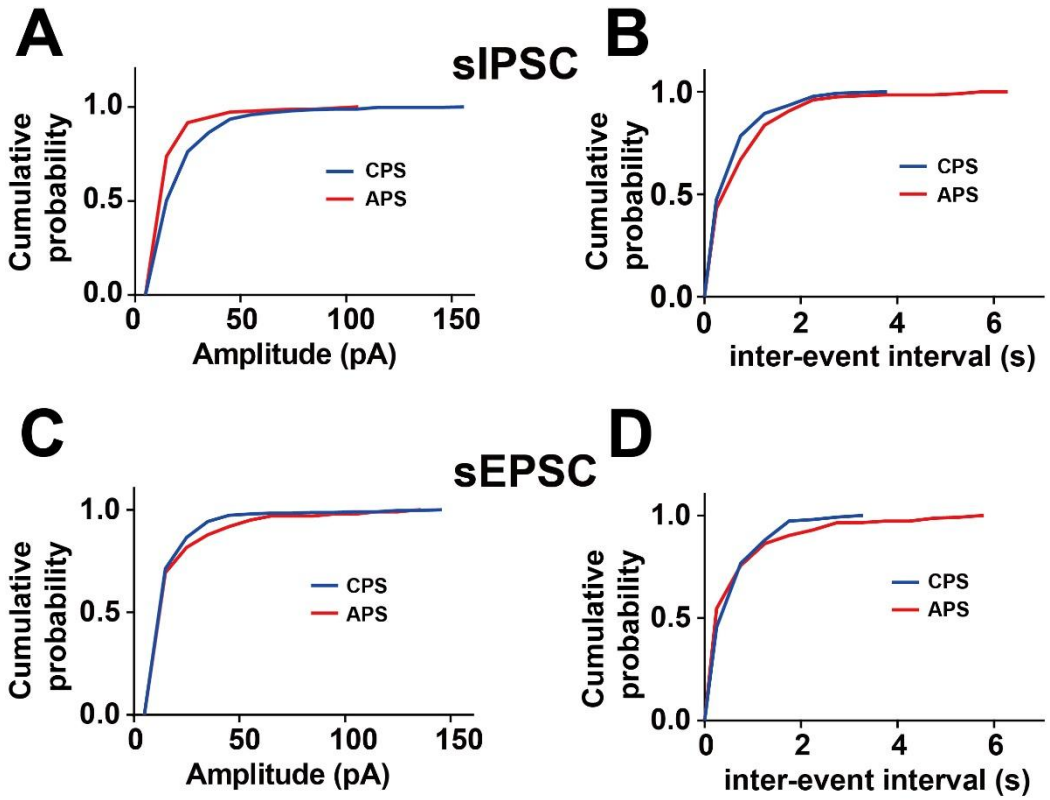

Fig. S10. Comparison of electrophysiological property of PFC neurons between CPS and APS. sIPSC cumulative probability of amplitude *(A)* and inter-event intervals *(B)* showed no differences between CPS (blue line) and APS (red line). sEPSC cumulative probability of amplitude *(C)* and inter-event intervals *(D)* showed no differences between CPS (blue line) and APS (red line).

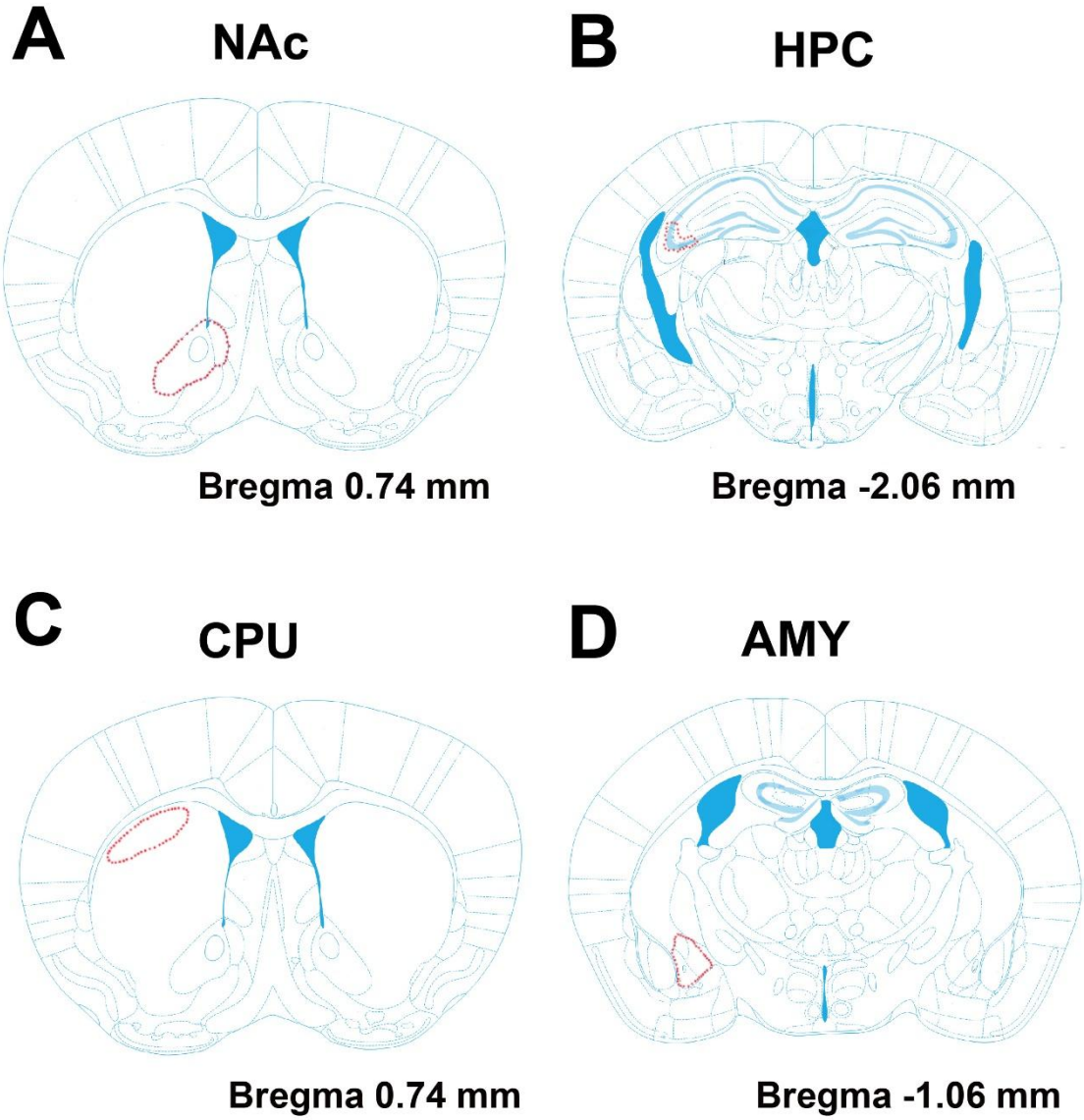

Fig. S11. Diagram of acute coronal brain slices for sampling experiment. The red dot line boxed areas show sampling locations from four brain regions. *(A)* NAc, nucleus accumbens; *(B)* HPC, hippocampus; *(C)* CPU, dorsal striatum; *(D)* AMY, amygdala. All the diagrams were modified with permission from The Mouse Brain in Stereotaxic Coordinates, 3rd edition, Keith B.J. Franklin and George Paxinos.

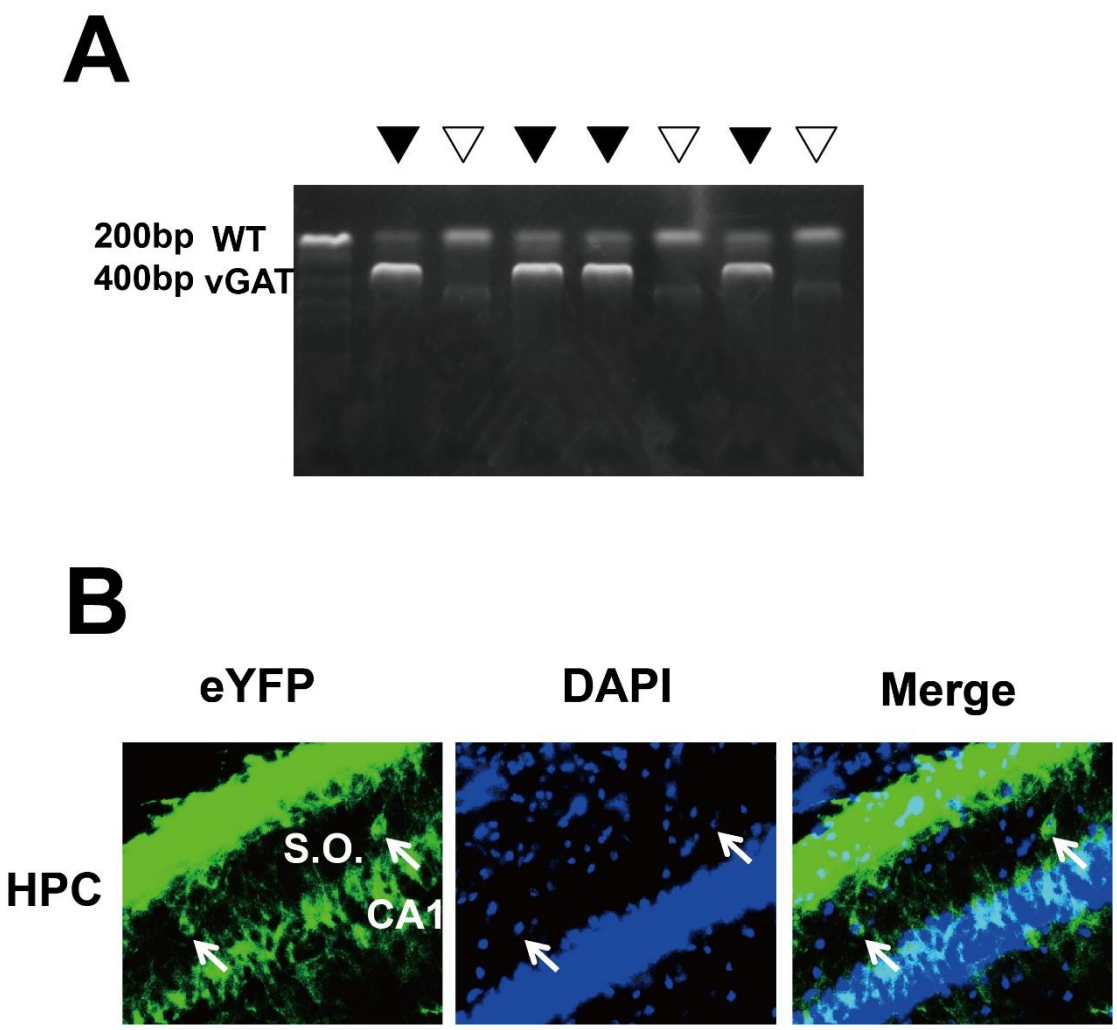

Fig. S12. Identification of VGAT-ChR$_2$ (H134R)-EYFP BAC transgenic mice and GABA expressing interneurons in Hippocampus. *(A)* Genotyping analysis of VGAT-ChR2 (H134R)-EYFP BAC transgenic mice. WT, wild-type locus; vGAT, VGAT-ChR2 locus; filled inverted triangles, vGAT; open inverted triangles, WT. *(B)* Only interneurons (arrowheads) in the stratum oriens region expressed eYFP. S.O., stratum oriens.

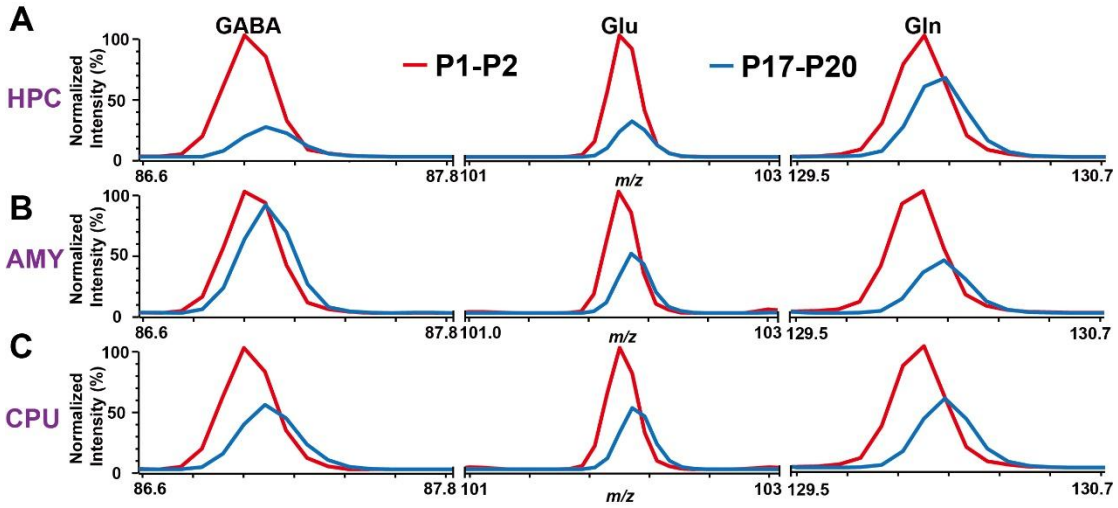

Fig. S13. Typical MS/MS spectra of GABA, Glu and Gln in single neurons of various brain areas including HPC *(A)*, AMY *(B)* and CPU *(C)* at ages of P1-P2 (red line) and P17-P20 (blue line).

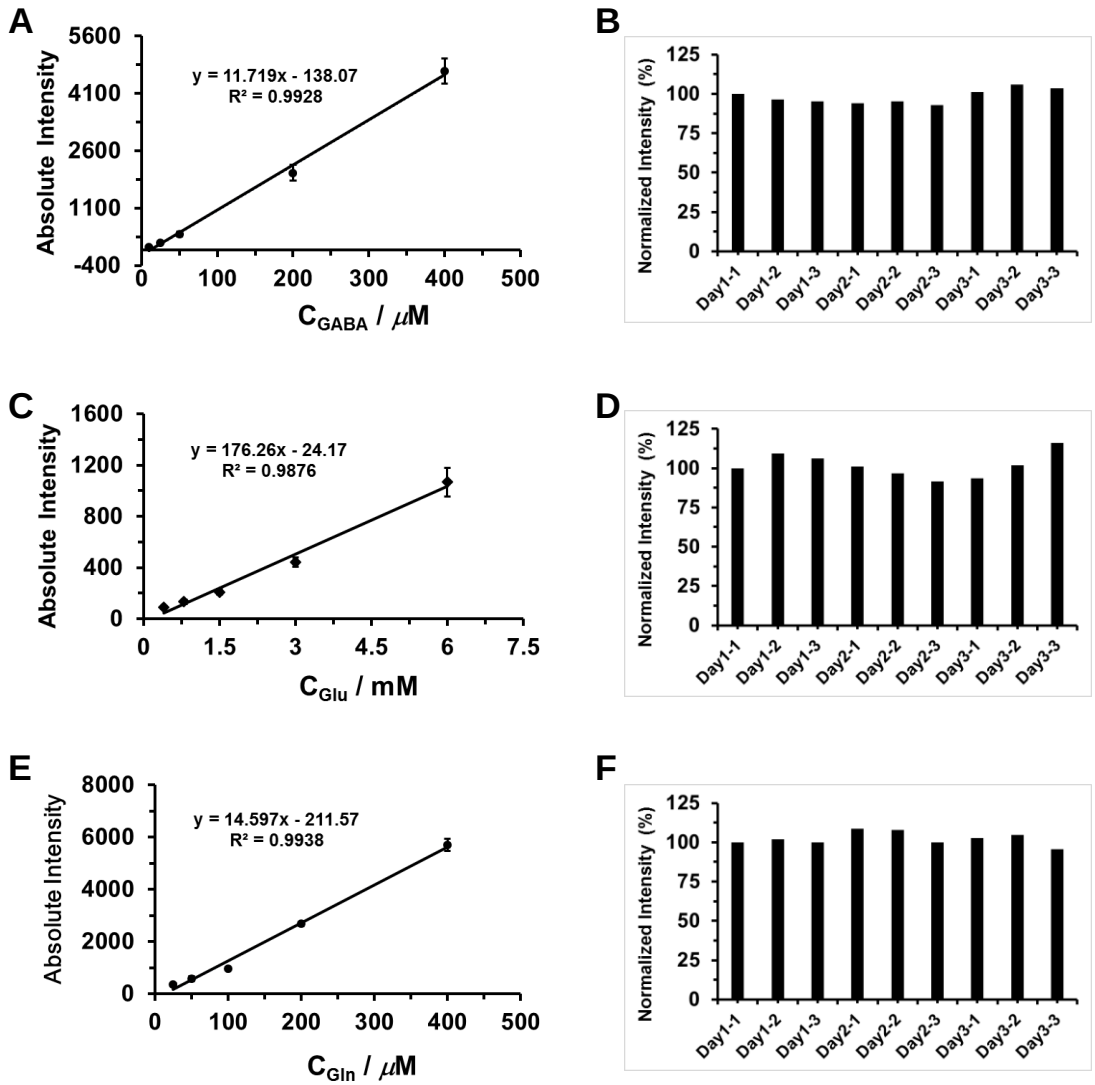

Fig. S14. Calibration curve of *(A)* GABA, *(C)* Glu and *(E)* Gln, with nine repeated measurement in continuous 3 days to illustrate the reproducibility of the present method for *(B)* GABA, *(D)* Glu and *(F)* Gln. GABA, Glu and Gln levels were found to be linear with MS intensity in the ranges we tested (GABA 10-400 μM, Gln 0.4-6 mM and Glu 25-400 μM). Repeated measurements were conducted at the level of 25 μM for GABA, 2 mM for Glu and 100 μM for Gln. All above calibration with external standards were obtained with artificial intracellular solution: potassium gluconate 130 mM, NaCl 6 mM, EGTA 11 mM, HEPES 10 mM, $CaCl_2$ 1 mM, NaOH 4 mM, $MgCl_2$ 1mM, Mg-ATP 2 mM and Na-GTP 0.2 mM (pH was adjusted to 7.3; osmolality was adjusted to 296 mOsm kg^{-1} with sucrose). Interday RSDs for GABA was 2.94, 1.23 and 2.25% with three continious days. Interday RSDs for Glu was 4.51, 4.82 and 10.92% with three continious days. Interday RSDs for Gln was 1.10, 4.58 and 4.64% with three continious days. Intraday RSDs for GABA, Glu and Gln were calculated to be 4.82, 4.67 and 2.68%, respectively.

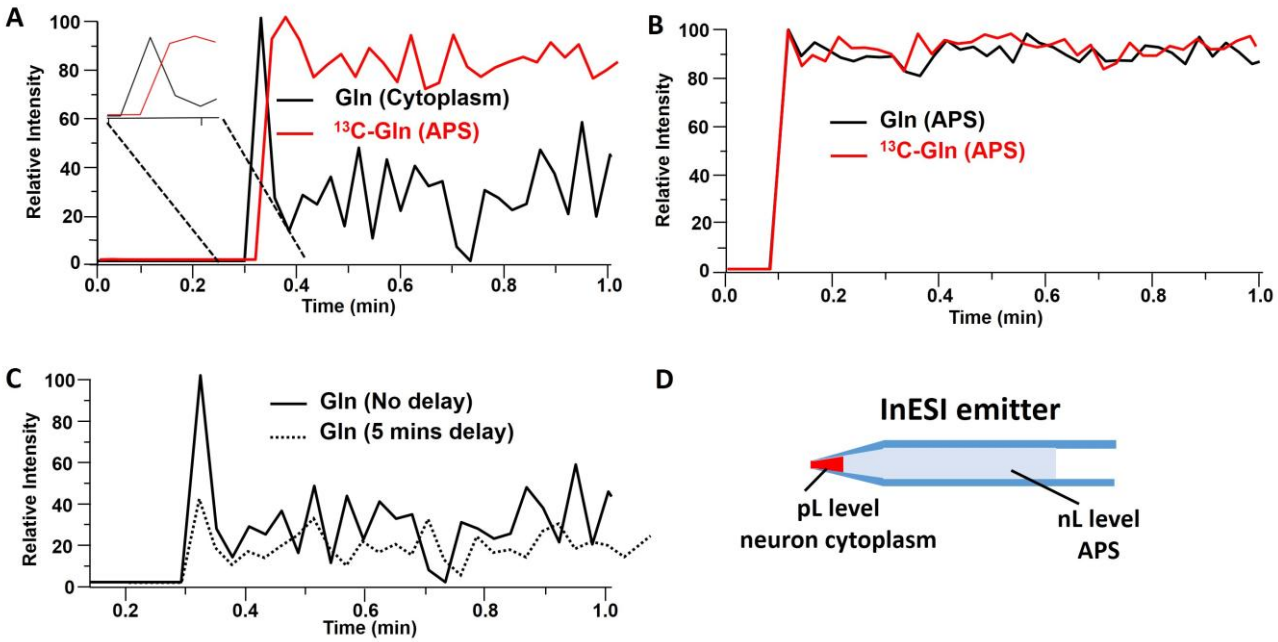

Fig. S15. Chromatogram of Glutamine (Gln) with 1,2-$^{13}C_2$-Gln added into APS as internal standards. *(A)* The mass spectrometry data showing different appearance time of Gln from neuronal cytoplasm and 1,2-$^{13}C_2$-Gln from APS. *(B)* The mass spectrometry data showing almost simultaneous appearance of Gln and 1,2-$^{13}C_2$-Gln which were pre-mixed in the APS. *(C)* Compare measurements of cytoplasm with no delay and 5 mins delay (the pipette was set still at room temperature for 5 mins after sample collection). *(D)* Scheme diagram of the possible spatial distribution of cytoplasm and APS.

As shown in **Fig. S15**, 1,2-$^{13}C_2$-Glutamine (1,2-$^{13}C_2$-Gln, 100 μM), as internal standard, was added into APS. While we conduct the experiments right after cytoplasm was collected, we found that maximum intensity of cytoplasm constituents (Gln) and internal standard (1,2-$^{13}C_2$-Gln) always appeared at different times. The signal of 1,2-$^{13}C_2$-Gln became stable until the disappearance of Gln signal (**Fig. S15*A***). However, the signals of Gln and 1,2-$^{13}C_2$-Gln were observed at the same time when the Gln (100 μM) and 1,2-$^{13}C_2$-Gln (100 μM) have been pre-mixed into the APS (**Fig. S15*B***). These results suggest that 1,2-$^{13}C_2$-Gln was not well mixed with the cytoplasm of neurons, which cannot be used as internal standard to solve the sampling issue. One alternative way is to wait long enough after cytoplasm collection to ensure thorough mixing of 1,2-$^{13}C_2$-Gln with cytoplasm. So the pipette was set still at room temperature for 5 mins after sample collection. However, the signal level of Gln decreased dramatically (**Fig. S15*C***), possibly due to the large dilution ratio or decomposition of cytoplasm. We thus speculate that the signal of the analyte came from the cytoplasm we collected from neurons. These cytoplasm remains at the top part of the spray tip, however the internal standard we spike into the APS remains at the end part of the tip (**Fig. S15*D***).

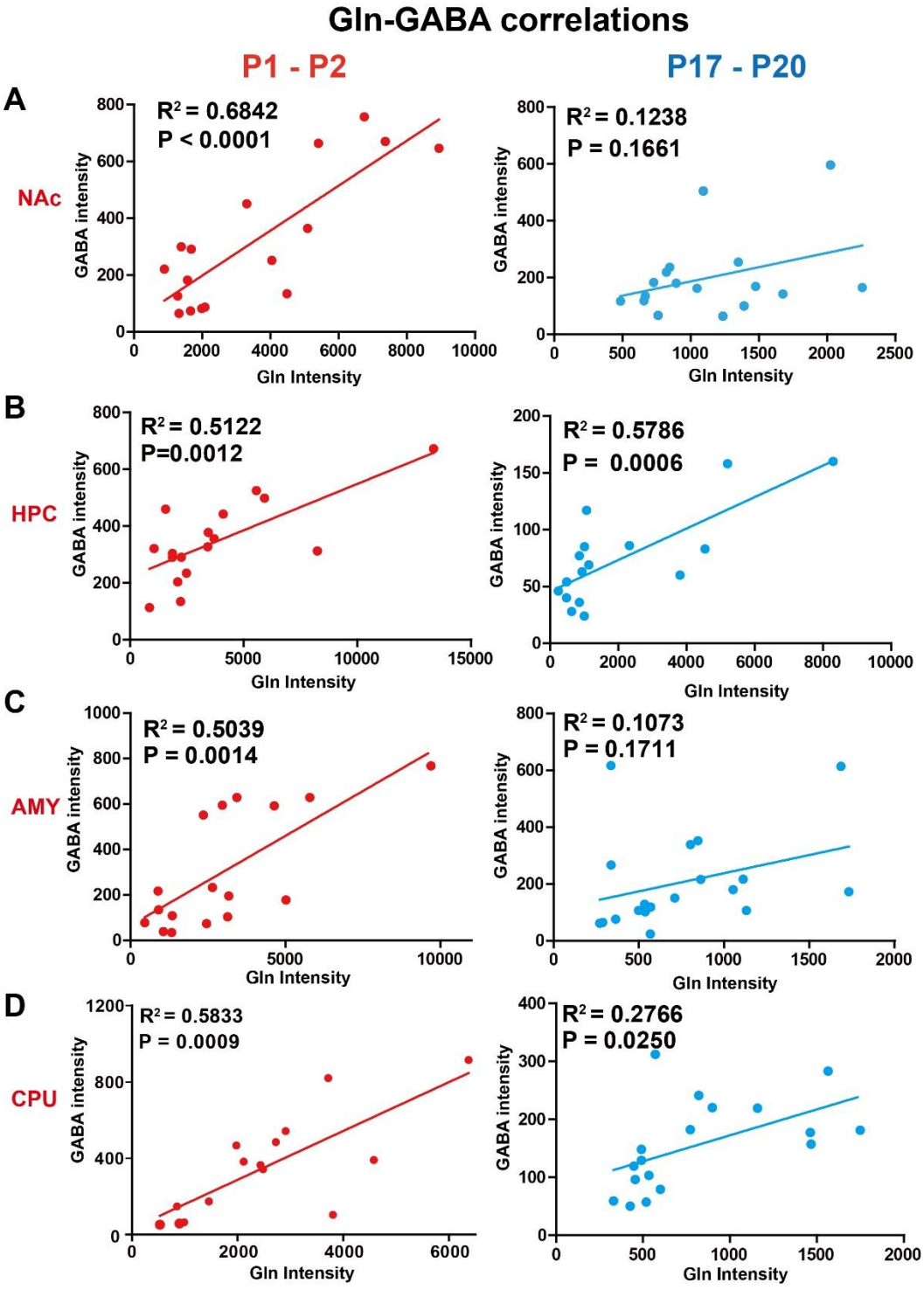

Fig. S16. The relationship between the single neuronal levels of Gln and GABA at ages of P1-P2 (red dots) and P17-P20 (blue dots) in variable brain areas including NAc *(A)*, HPC *(B)*, AMY *(C)* and CPU *(D)* of three mice.

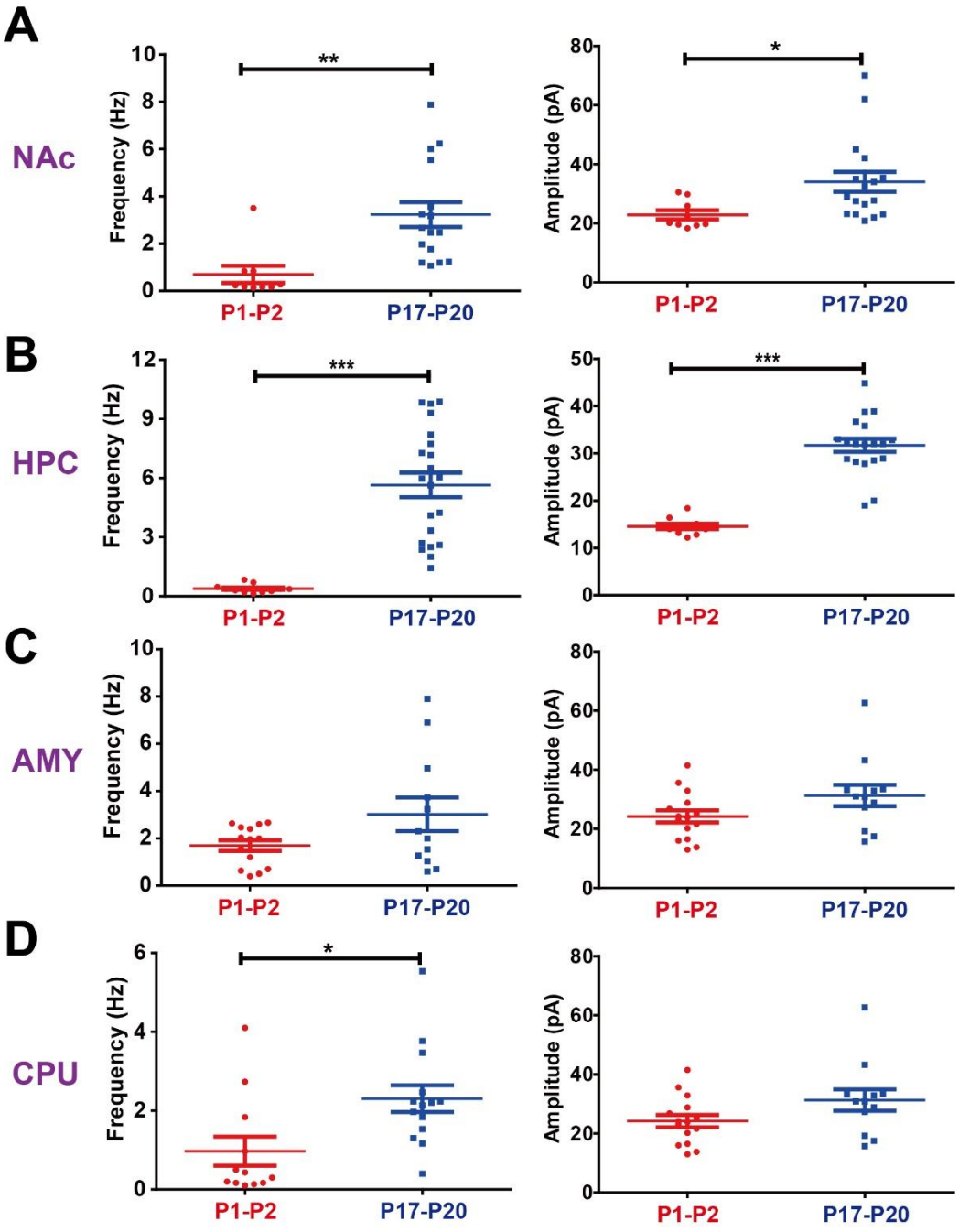

Fig. S17. Comparison of spontaneous neuronal firing activity between neonatal and young mice. Frequency and amplitude of postsynaptic current of *(A)* NAc , *(B)* HPC, *(C)* AMY and *(D)* CPU neurons from 3 mice showed lower firing activity at ages of P1-P2 (red dots) than P17-P20 (blue dots).

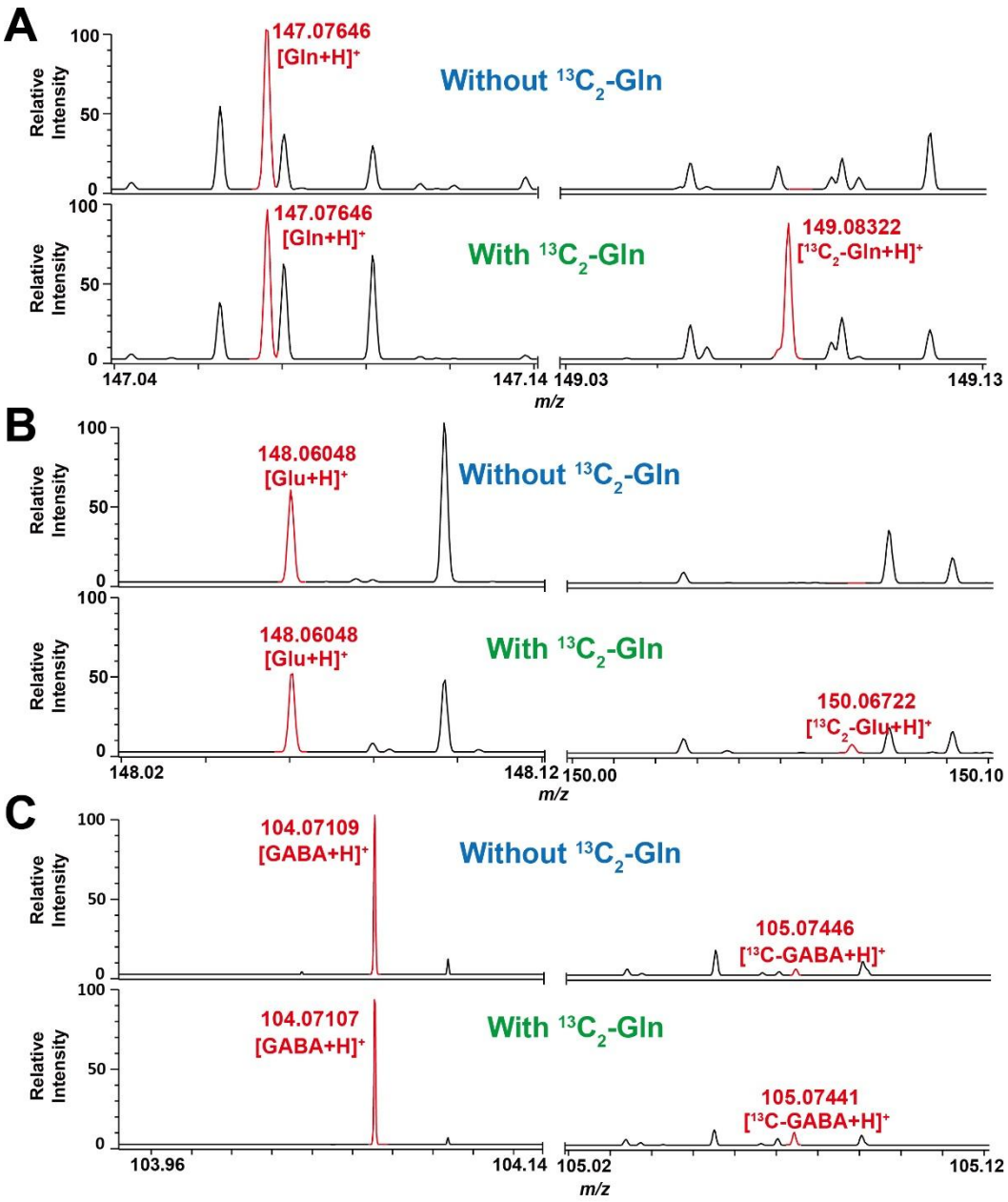

Fig. S18. Typical MS spectra of Gln and $^{13}C_2$-Gln *(A)*, Glu and $^{13}C_2$-Glu *(B)*, and GABA and ^{13}C-GABA *(C)* in the single neurons of nucleus accumbens (NAc) without or with incubation of 1,2-$^{13}C_2$-Gln (0.4 mM).

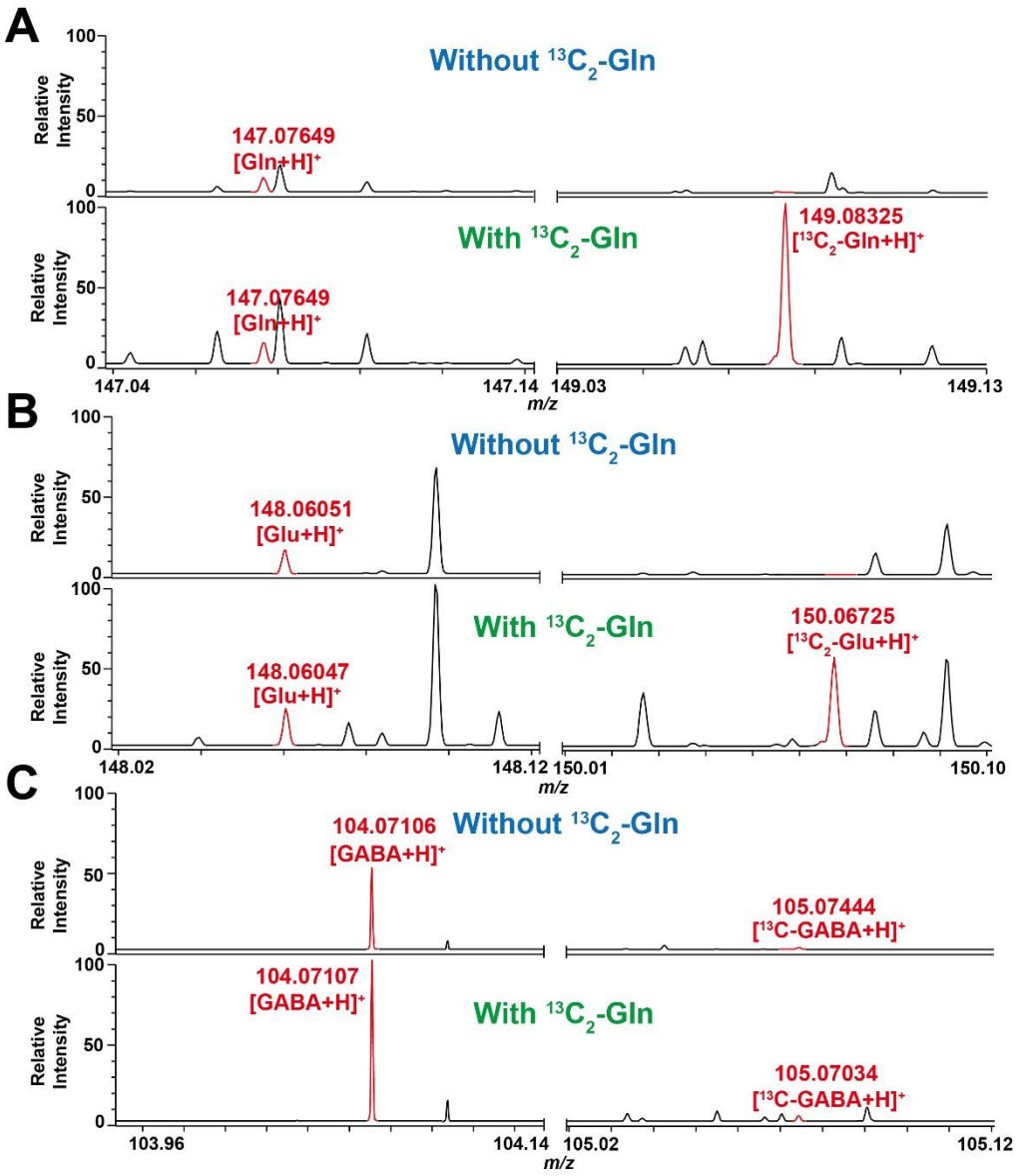

Fig. S19. Typical MS spectra of Gln and $^{13}C_2$-Gln *(A)*, Glu and $^{13}C_2$-Glu *(B)*, and GABA and ^{13}C-GABA ***(C)*** in the single neurons of hippocampus (HPC) without or with incubation of 1,2- $^{13}C_2$-Gln (0.4 mM).

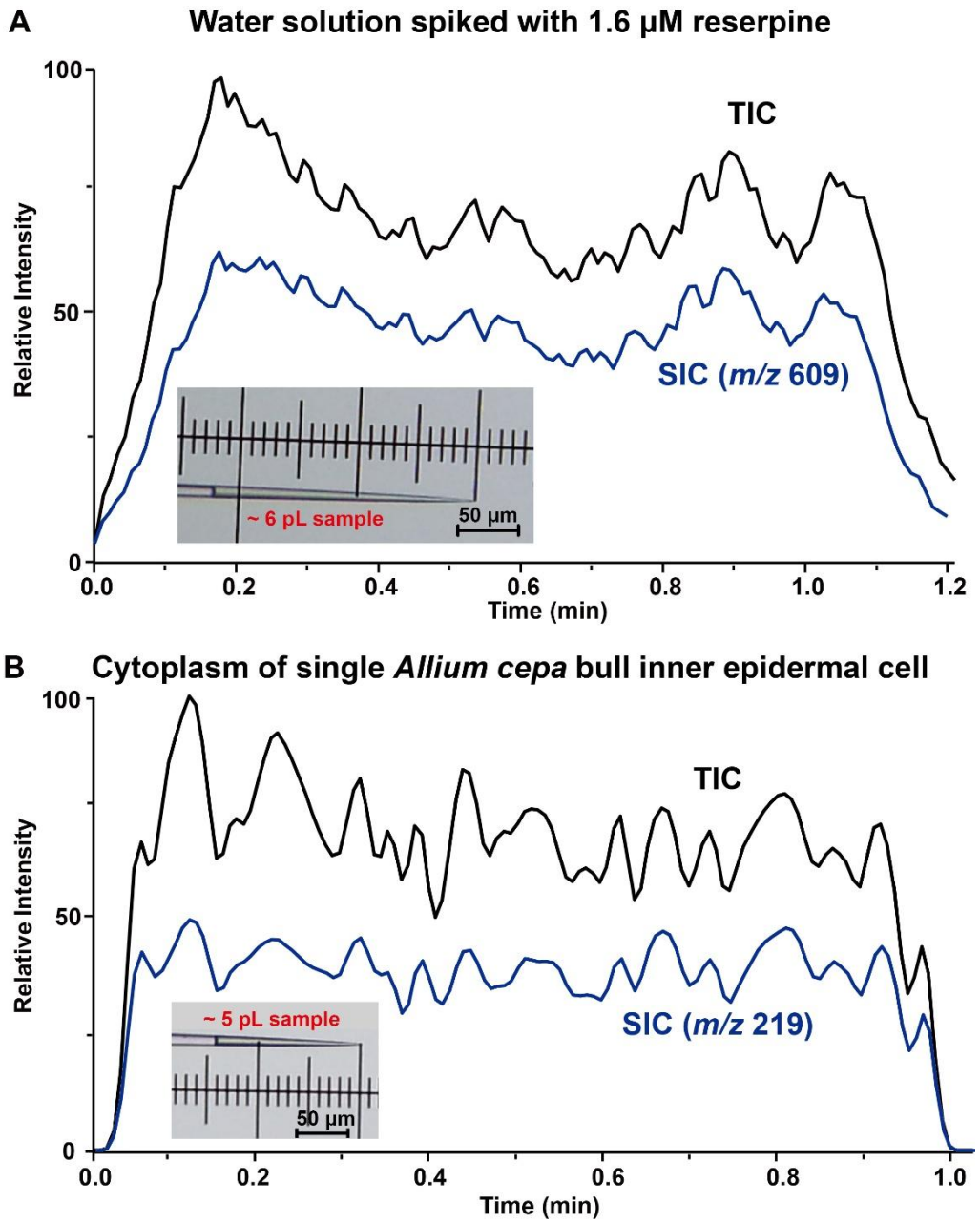

Fig. S20. The flow rate of ~ 5 pL/min was obtained using InESI. *(A)* Total ion chromatogram (TIC, black line) and selected ion chromatogram (SIC, blue line) of protonated reserpine obtained with ~ 6 pL water solution spiked with 1.6 µM reserpine subjected to InESI. Insert: real image of water solution volume. *(B)* Total ion chromatogram (TIC, black line) and selected ion chromatogram (SIC, blue line) of potassium adduct hexose obtained with ~ 5 pL cytoplasm of *Allium cepa* bull inner epidermal single cell subjected to InESI. Insert: real image of cytoplasm volume.

Table S1. List of A. cepa bulb epidermal cells metabolites

No.	Observed mass, *m/z*	Theoretical, *m/z*	Error, ppm	Formula	Tentative assignment	Cell type
1	104.10722	104.10754	3.07	$[C_5H_{13}N+H]^+$	Neurine	Outer
2	108.08118	108.08132	1.30	$[C_7H_9N+H]^+$	Benzylamine	Inner/Outer
3	175.11866	175.11950	4.80	$[C_6H_{14}N_4O_2+H]^+$	Arginine	Inner/Outer
4	178.05291	178.05379	4.94	$[C_6H_{11}NO_3S+H]^+$	alliin	Inner/Outer
5	198.09690	198.09776	4.34	$[C_6H_{12}O_6+NH_4]^+$	Hexose	Inner/Outer
	203.05218	203.05316	4.83	$[C_6H_{12}O_6+Na]^+$		Inner/Outer
	219.02610	219.02710	4.57	$[C_6H_{12}O_6+K]^+$		Inner/Outer
6	200.03488	200.03573	4.25	$[C_6H_{11}NO_3S+Na]^+$	N-formyl-L-methionine	Outer
	216.00876	216.00967	4.21	$[C_6H_{11}NO_3S+K]^+$		Outer
7	253.03789	253.03772	-0.67	$[C_7H_{14}NO_3S_3+H]^+$	unknown	Outer
	275.01972	275.01966	-0.22	$[C_7H_{14}NO_3S_3+Na]^+$		Outer
	290.99370	290.99360	-0.34	$[C_7H_{14}NO_3S_3+K]^+$		Outer
8	365.10457	365,10598	3.86	$[C_{12}H_{22}O_{11}+Na]^+$	Disaccharide (2 hexose units)	Inner/Outer
	381.07853	381.07992	3.65	$[C_{12}H_{22}O_{11}+K]^+$		Inner/Outer
9	527.15724	527.15881	2.98	$[C_{18}H_{32}O_{16}+Na]^+$	Triaccharide (3 hexose units)	Inner/Outer
	543.13121	543.13275	2.84	$[C_{18}H_{32}O_{16}+K]^+$		Inner/Outer
10	689.20985	689.21163	2.58	$[C_{24}H_{42}O_{21}+Na]^+$	Tetrasaccharide (4 hexose units)	Inner/Outer
11	705.18347	705.18557	2.98	$[C_{24}H_{42}O_{21}+K]^+$		Inner/Outer
12	851.26225	851.26446	2.60	$[C_{30}H_{52}O_{26}+Na]^+$	Pentasaccharide (5 hexose units)	Inner/Outer
	867.23587	867.23840	2.92	$[C_{30}H_{52}O_{26}+K]^+$		Inner/Outer
13	1013.31458	1013.31728	2.66	$[C_{36}H_{62}O_{31}+Na]^+$	Hexasaccharide (6 hexose units)	Inner/Outer
	1029.28835	1029.29112	2.69	$[C_{36}H_{62}O_{31}+K]^+$		Inner/Outer
14	1175.36771	1175.37011	2.04	$[C_{42}H_{72}O_{36}+Na]^+$	Heptasaccharide (6 hexose units)	Inner/Outer
	1191.34169	1191.34405	1.98	$[C_{42}H_{72}O_{36}+K]^+$		Inner/Outer

The assignment of chemical composition is based on accurate mass measurements, comparison of isotopic patterns, information found in databases, such as the Plant Metabolic Network database (http://plantcyc.org/), and some previous related literatures

Table S2. List of metabolites obtained from single neuro of mouse brain tissue

No.	Observed mass, *m/z*	Theoretical, *m/z*	Error, ppm	Formula	Tentative assignment
1	76.04003	76.03985	-0.25	$[C_2H_5NO_2+H]^+$	Glycine
2	90.05554	90.05550	-0.44	$[C_3H_7NO_2+H]^+$	Alanine
3	104.07108	104.07115	0.67	$[C_4H_9NO_2+H]^+$	Gamma-aminobutyric acid (GABA)
4	104.10745	104.10754	0.86	$[C_5H_{13}NO+H]^+$	choline
5	106.05032	106.05042	0.94	$[C_3H_7NO_3+H]^+$	serine
6	114.05532	114.05550	1.58	$[C_5H_7NO_2+H]^+$	1-Pyrroline-5-carboxylic acid
7	116.07095	116.07115	1.72	$[C_5H_9NO_2+H]^+$	proline
8	118.08657	118.08680	1.95	$[C_5H_{11}NO_2+H]^+$	L-Valine Glycine betaine
9	120.06582	120.06607	2.08	$[C_4H_9NO_3+H]^+$	Threonine
10	124.03960	124.03985	2.02	$[C_6H_5NO_2+H]^+$	Picolinic acid
11	130.05004	130.05042	2.92	$[C_5H_7NO_3+H]^+$	Pyrrolidonecarboxylic acid (5-oxo-proline) 1-Pyrroline-4-hydroxy-2-carboxylate
12	132.06568	132.06607	2.95	$[C_5H_9NO_3+H]^+$	Glutamic gamma-semialdehyde
13	132.10106	132.10245	2.95	$[C_6H_{13}NO_2+H]^+$	Leucine Isoleucine
14	134.04492	134.04533	3.06	$[C_4H_7NO_4+H]^+$	Aspartic acid
15	139.05029	139.05075	3.31	$[C_6H_6N_2O_2+H]^+$	Urocanic acid
16	141.09107	141.09156	3.47	$[C_8H_{12}O_2+H]^+$	2-Propyl-2,4-pentadienoic acid
17	142.12275	142.12319	3.10	$[C8\ H15\ O\ N+H]^+$	Conhydrinone
18	146.11760	146.11810	3.42	$[C_7H_{16}NO_2]^+$	Acetylcholine
19	147.07654	147.07697	2.92	$[C_5H_{10}N_2O_3+H]^+$	Glutamine
20	148.06048	148.06098	3.38	$[C_5H_9NO_4+H]^+$	Glutamate
21	154.08629	154.08680	3.31	$[C_8H_{11}NO_2+H]^+$	Dopamine
22	155.10669	155.10720	3.29	$[C_9H_{14}O_2+H]^+$	xi-2,2,6-Trimethyl-1,4-cyclohexanedione
23	156.07688	156.07730	2.69	$[C_6H_9N_3O_2+H]^+$	L-Histidine
24	156.10198	156.10245	3.01	$[C_8H_{13}NO_2+H]^+$	Arecoline
25	159.06525	159.06573	3.02	$[C_7H_{10}O_4+H]^+$	Succinylacetone
26	160.06054	160.06098	2.75	$[C_6H_9NO_4+H]^+$	L-2-Amino-4-methylenepentanedioic acid
27	160.09689	160.09737	3.00	$[C_7H_{13}NO_3+H]^+$	Methyl 5-(hydroxymethyl)pyrrolidine-3-carboxylate
28	164.07064	164.07115	3.11	$[C_9H_9NO_2+H]^+$	3-Methyldioxyindole
29	166.08633	166.08680	2.83	$[C_9H_{11}NO_2+H]^+$	L-Phenylalanine
30	168.10196	168.10245	2.91	$[C_9H_{13}NO_2+H]^+$	Phenylephrine

					3-Methoxytyramine
31	170.08123	170.08172	2.88	$[C_8H_{11}NO_3+H]^+$	6-Hydroxydopamine 5-Hydroxydopamine Pyridoxine 6-Acetyl-2,3-dihydro-2-(hydroxy methyl)-4(1H)-pyridinone Norepinephrine (Noradrenaline)
32	170.11765	170.11810	2.65	$[C_9H_{15}NO_2+H]^+$	Homoarecoline
33	175.09660	175.09704	2.51	$[C_8H_{14}O_4+H]^+$	Suberic acid
34	176.09180	176.09228	2.72	$[C_7H_{13}NO_4+H]^+$	N-Carboxyethyl-g-aminobutyric acid
35	180.06556	180.06607	2.83	$[C_9H_9NO_3+H]^+$	Adrenochrome
36	181.04955	181.05009	2.98	$[C_9H_8O_4+H]^+$	4-Hydroxyphenylpyruvic acid
37	182.08128	182.08172	2.42	$[C_9H_{11}NO_3+H]^+$	Tyrosine
38	182.10246	182.10419	9.50	$[C_7H_{11}N_5O+H]^+$	6-Methyltetrahydropterin
39	184.09691	184.09737	2.50	$[C_9H_{13}NO_3+H]^+$	Epinephrine Normetanephrine 3,4,5,6-Tetrahydrohippuric acid
40	185.08120	185.08170	2.70	$[C_5H_{15}NO_4P+H]^+$	Phosphorylcholine
41	204.12315	204.12358	2.10	$[C_9H_{17}NO_4+H]^+$	L-Acetylcarnitine
42	208.06088	208.06098	0.48	$[C_{10}H_9NO_4+H]^+$	4-(2-Aminophenyl)-2,4-dioxobuta noic acid
43	208.09694	208.09737	2.07	$[C_{11}H_{13}NO_3+H]^+$	Phenylpropionylglycine N-Acetyl-L-phenylalanine
44	208.11800	208.11850	2.40	$[C_8H_{17}NO_5+H]^+$	Miglitol
45	222.09724	222.09776	2.34	$[C_8H_{15}NO_6+H]^+$	N-Acetylgalactosamine
46	227.16418	227.16472	2.38	$[C_{13}H_{22}O_3+H]^+$	4,5-Dihydrovomifoliol
47	232.11803	232.11850	2.02	$[C_{10}H_{17}NO_5+H]^+$	Suberylglycine
48	232.15433	232.15448	0.65	$[C_{11}H_{21}NO_4+H]^+$	Butyrylcarnitine
49	260.18560	260.18618	2.23	$[C_{13}H_{25}NO_4+H]^+$	Hexanoylcarnitine
50	260.22196	260.22123	-2.81	$[C_{12}H_{25}N_3O_3+H]^+$	Lysyl-Leucine Isoleucyl-Lysine Leucyl-Lysine Lysyl-Isoleucine
51	274.20106	274.20183	2.81	$[C_{14}H_{27}NO_4+H]^+$	Heptanoylcarnitine
52	275.23688	275.23749	2.22	$[C_{19}H_{30}O+H]^+$	Androstenol
53	276.14416	276.14471	1.99	$[C_{12}H_{21}NO_6+H]^+$	Glutarylcarnitine
54	276.18057	276.18110	1.92	$[C_{13}H_{25}NO_5+H]^+$	Hydroxyhexanoycarnitine

The assignment of chemical composition is based on accurate mass measurements, comparison of isotopic patterns, information found in databases, such as Human metabolome database (http://www.hmdb.ca/), and some previous related literatures.